UvA-DARE (Digital Academic Repository)

Divertor conditions relevant for fusion reactors achieved with linear plasma generator

van Eck, H.J.N.; Kleijn, A.W.; Lof, A.; van der Meiden, H.J.; van Rooij, G.J.; Scholten, J.; Zeijlmans van Emmichoven, P.A.

[Link to publication]

Divertor conditions relevant for fusion reactors achieved with linear plasma generator

H. J. N. van Eck, A. W. Kleyn, A. Lof, H. J. van der Meiden, G. J. van Rooij et al.

Related Articles

On the toroidal plasma rotations induced by lower hybrid waves
Phys. Plasmas 20, 022502 (2013)

Comparing linear ion-temperature-gradient-driven mode stability of the National Compact Stellarator Experiment and a shaped tokamak
Phys. Plasmas 20, 022305 (2013)

Quick asymptotic expansion aided by a variational principle
Phys. Plasmas 20, 024504 (2013)

Ion temperature gradient instability at sub-Larmor radius scales with non-zero ballooning angle
Phys. Plasmas 20, 022101 (2013)

Nonlinear canonical gyrokinetic Vlasov equation and computation of the gyrocenter motion in tokamaks
Phys. Plasmas 20, 012515 (2013)

Additional information on Appl. Phys. Lett.

Journal Homepage: http://apl.aip.org/

Journal Information: http://apl.aip.org/about/about_the_journal

Top downloads: http://apl.aip.org/features/most_downloaded

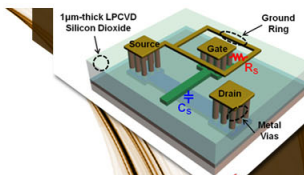Information for Authors: http://apl.aip.org/authors

Divertor conditions relevant for fusion reactors achieved with linear plasma generator

H. J. N. van Eck,[1,a)] A. W. Kleyn,[1,2] A. Lof,[1] H. J. van der Meiden,[1] G. J. van Rooij,[1] J. Scholten,[1] and P. A. Zeijlmans van Emmichoven[1]

[1]FOM Institute DIFFER - Dutch Institute For Fundamental Energy Research, Association EURATOM-FOM, Trilateral Euregio Cluster, P.O. Box 1207, 3430 BE Nieuwegein, The Netherlands
[2]Van 't Hoff Institute for Molecular Sciences, Faculty of Science, University of Amsterdam, P.O. Box 94157, 1090 GD Amsterdam, The Netherlands

Intense magnetized hydrogen and deuterium plasmas have been produced with electron densities up to $3.6 \times 10^{20} \, \text{m}^{-3}$ and electron temperatures up to $3.7 \, \text{eV}$ with a linear plasma generator. Exposure of a W target has led to average heat and particle flux densities well in excess of $4 \, \text{MW} \, \text{m}^{-2}$ and $10^{24} \, \text{m}^{-2} \, \text{s}^{-1}$, respectively. We have shown that the plasma surface interactions are dominated by the incoming ions. The achieved conditions correspond very well to the projected conditions at the divertor strike zones of fusion reactors such as ITER. In addition, the machine has an unprecedented high gas efficiency. [http://dx.doi.org/10.1063/1.4768302]

The magnetic topology of fusion devices such as ITER guides the heat and particles from the plasma towards an area called the divertor. Close to the divertor, the electron density n_e in the plasma is very high and amounts to $\sim 10^{20}$–$10^{21} \, \text{m}^{-3}$ at an electron temperature T_e of 1–5 eV, leading to time-averaged particle and energy flux densities of $10^{24} \, \text{m}^{-2} \, \text{s}^{-1}$ and $10 \, \text{MW} \, \text{m}^{-2}$, respectively.[1,2] On top of that, magneto-hydrodynamic instabilities in the plasma edge, commonly called edge localized modes (ELMs),[3] can deposit an esti-mated 2–4 GW m^{-2} for 0.5–1 ms on these divertor strike zones. These extreme particle and heat fluxes place severe demands on the material surfaces and challenge our ability to control and predict plasma-surface interactions (PSI). The densities and fluxes are so high that the system has entered the so-called strongly coupled regime, where molecules and dust particles that come off the surface are confined and remain part of the PSI system. The wall material will erode and possi-bly even melt, thereby endangering the durability of the wall elements and the condition to maintain a very clean and pure plasma. Due to the major (3 orders of magnitude in terms of ion fluence) up scaling between ITER and current magnetic confinement devices, the need has arisen to study these effects in a well-controlled and systematical way. Dedicated toka-maks and linear devices are needed, where the key question is if they can enter the ITER relevant regime in terms of density, temperature, degree of ionization, and background pressure. Linear plasma simulators benefit from better accessibility, but have to cope with the fact that intense plasma at low tempera-ture can only be made by sources that co-exhaust large quanti-ties of neutral gas.

A linear machine designed specifically to reach the ITER relevant regime is Magnum-PSI (MAgnetized plasma Generator and NUMerical modeling for PSI). A quasi steady-state axial magnetic field up to 1.9 T is generated to confine a high density, low temperature plasma of a wall sta-bilized dc cascaded arc[4–6] to an intense magnetized plasma

beam directed on a target. As opposed to its forerunner Pilot-PSI, the present experiment uses a differentially pumped vacuum system, where the vacuum vessel is divided into two chambers which are individually pumped by large roots pumps with pump speeds in the range of $20\,000 \, \text{m}^3 \, \text{h}^{-1}$. A design drawing of the setup is given in Fig. 1. A flow restriction (skimmer) between the two vacuum chambers keeps the neutral gas flow to the target region sufficiently low.[7] As such, the experiment combines the high ion flux capabilities of Pilot-PSI[8] with low background pressure and large beam diameter to reach the strongly coupled regime. It should be mentioned that differential pumping has been used before on linear plasma generators,[9–12] in which it was used to vary the neutral pressure in the target chamber by means of gas puff to study detached plasmas as a possible way to mitigate the power flux to the divertor. However, the electron density and fluxes in these machines were more than an order of magnitude lower as compared to the conditions at the
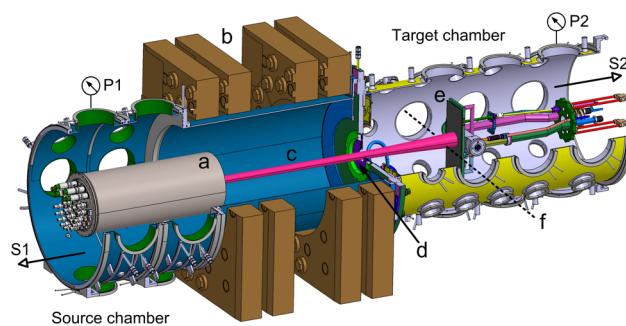
FIG. 1. Design drawing of the differentially pumped experiment. The source and target chamber are each pumped by their own pumping station (S1 and S2). The source chamber holds the plasma source, which is mounted inside a movable water cooled tube (a). The magnetic field coils (b) are positioned such that the magnetic field lines expand a factor of 2.6 before reaching the target. The magnetized plasma beam (c) flows through the skimmer (d) from source to target (e) while most of the neutrals are scraped off and pumped away. Thomson scattering yields n_e and T_e profiles directly in front of the target (f). The distance between the source and the target is 1 m. The skimmer opening is 50 mm in diameter. The target can be rotated around two orthogonal axes to vary the angle of incidence.

a)Electronic mail: h.j.n.vaneck@differ.nl.

ITER strike zones. In the present work, we show that ITER divertor conditions have been achieved in a linear machine together with an unprecedented high ionization efficiency.

The measurements presented here were performed with an electrically floating, W target in the perpendicular position with respect to the plasma beam as indicated in Fig. 1. n_e and T_e profiles have been determined with Thomson scattering (TS) 25 mm in front of the target with a spatial resolution of 1.6 mm.[13] The purity of the plasma just in front of the target was monitored with wide spectral range optical emission spectroscopy (OES). Temperature and flow sensors are installed inside the cooling circuits to enable calorimetric measurements with an accuracy of 10%. Fig. 2 shows the radial n_e and T_e profiles measured with the source running on 5 Pa m^3 s^{-1} H$_2$ and D$_2$ for a source current I_s of 225 A. The FWHM diameters of the beams are about 25 mm. For H$_2$, the maximum n_e amounts to 1.3×10^{20} m^{-3} at an T_e of 3.7 eV, for D$_2$ n_e rises to 3.6×10^{20} m^{-3} at an T_e of 2.0 eV. The lower n_e and higher T_e for H$_2$ as compared to D$_2$ were recorded for all source and field settings. The higher density for D$_2$ is partly attributed to the sonic flow condition at the exit of the source, i.e., a lower flow speed due to the higher mass. To understand the differences in detail, however, dedi-
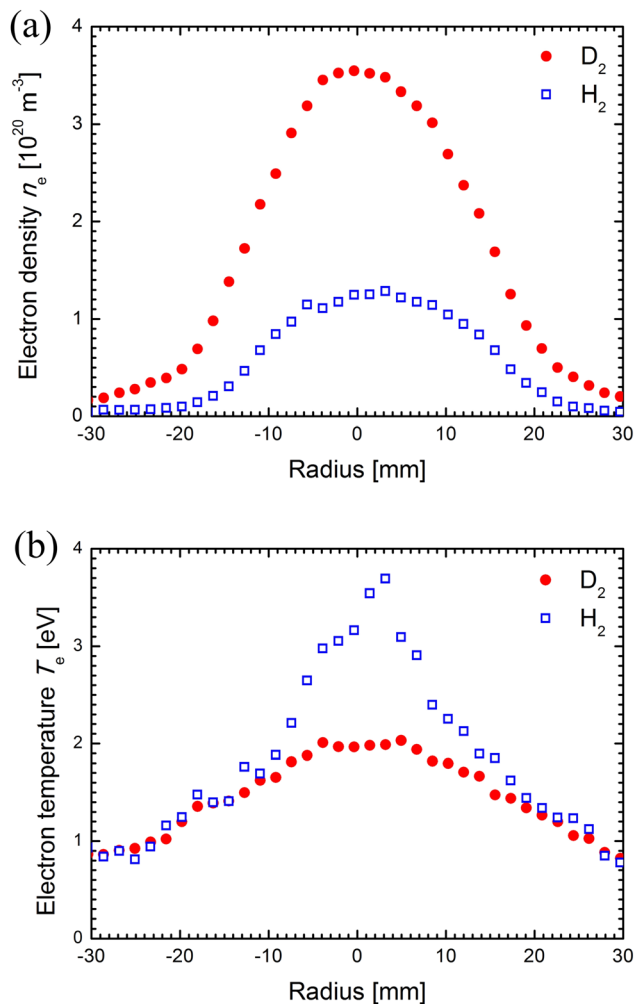
cated modeling will be required since the plasma production in the source as well as the transport to the target is different for the two species. For both gases, n_e and T_e are well within the regime relevant for the ITER divertor of 10^{20}–10^{21} m^{-3} and 1–5 eV, respectively.

During the experiments, the background pressures in the source and target chamber have been recorded at positions where the neutral gas is in thermal equilibrium with the water cooled vessel (see Fig. 1). The results for 5 Pa m^3 s^{-1} D$_2$ for several source currents and two magnetic field settings are shown in Fig. 3. The pressures in the source and target chambers without magnetic field are, respectively, 1.0 Pa and 0.2 Pa, independent of I_s (depicted with dashed/dashed-dotted lines in the figure). Upon application of the magnetic field and with increase of I_s, the pressure in the source chamber significantly drops, whereas the pressure in the target chamber rises by approximately the same amount.

Without magnetic field, the plasma forms a supersonic expansion in a neutral gas background with the shock position well before the skimmer. The on-axis ionization decreases quickly and almost no plasma enters the target chamber.[14] This means that virtually all of the gas flow in the target chamber arises from neutral background gas diffusing into the chamber via the skimmer. This gas flow (expressed in Pa m^3 s^{-1}) was determined by multiplying the pressure in the target chamber with the (measured, pressure dependent) effective pump speed (expressed in m^3 s^{-1}). The gas flows in the source and target chamber without magnetic field correspond to, respectively, 85% and 15% of the total gas flow. Turning the magnetic field on has two effects: (1) the plasma source efficiency increases due to the lower radial heat loss causing n_e to increase and (2) the ionized particles are confined to a magnetized beam with a diameter smaller than the skimmer opening. As a result, the ionized particles are transported from the source to the target chamber, where they are neutralized at the target plate and contribute to the neutral gas load in the target chamber. Increasing I_s increases n_e and the amount of transported ions. The resulting total particle flux to the target chamber Γ_p, as deduced from the

FIG. 2. Radial electron density n_e (a) and electron temperature T_e (b) profiles. The H$_2$ and D$_2$ flow was 5 Pa m^3 s^{-1} and the magnetic field was 0.87 T at the source and 0.15 T at the TS position. Source current I_s was set at 225 A.
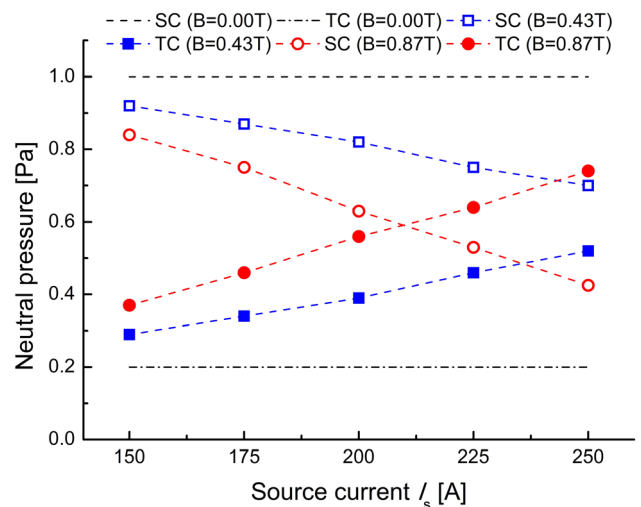

FIG. 3. Neutral pressure in the source chamber (SC) and target chamber (TC) as a function of source current I_s for no applied magnetic field as well as for magnetic fields of 0.43 T and 0.87 T. The D$_2$ flow was 5 Pa m^3 s^{-1}. Dashed lines between the data points to guide the eye only.

gas flow measurements and assuming the gas behaving as an ideal gas, is presented in Fig. 4(a). Although their n_e and T_e profiles are quite different, the H and D fluxes are strikingly equal. Γ_p increases as a function of source current and magnetic field to a maximum of $1.9 \times 10^{21}\,\mathrm{s}^{-1}$. Γ_p without magnetic field is constant at $4.0 \times 10^{20}\,\mathrm{s}^{-1}$ for D_2 and $4.1 \times 10^{20}\,\mathrm{s}^{-1}$ for H_2. Note that this method cannot distinguish between ions and neutrals.

In addition to the pressure measurements, calorimetry on the target cooling water was carried out. From the results, the total plasma flux on the target can be deduced by taking the ratio of the calorimetric power and an estimated average energy $\hat{E}_{pair}$ deposited by an electron-ion pair. For a drifting Maxwellian velocity distribution,[15] $\hat{E}_{pair}$ would be the forward power flux plus the ionization energy of the ion plus half the dissociation energy, i.e., $\hat{E}_{pair} = 5/2\ kT_e + 5/2\ kT_i + 1/2\ mv_i^2 + E_{ionization} + 1/2\ E_{dissociation}$. This formula would hold for the situation where the ions are all absorbed by the target, where they neutralize and recombine to molecules. In fact, it is known that a significant fraction of the ions reflect from the target, for H on W approximately 60%,[16] thereby taking with them a large part of their kinetic energy and not releasing the dissociation energy. We, therefore, corrected the above formula by including only 40% of the kinetic energy of the ions as well as only 40% of the dissociation energy. The ioniz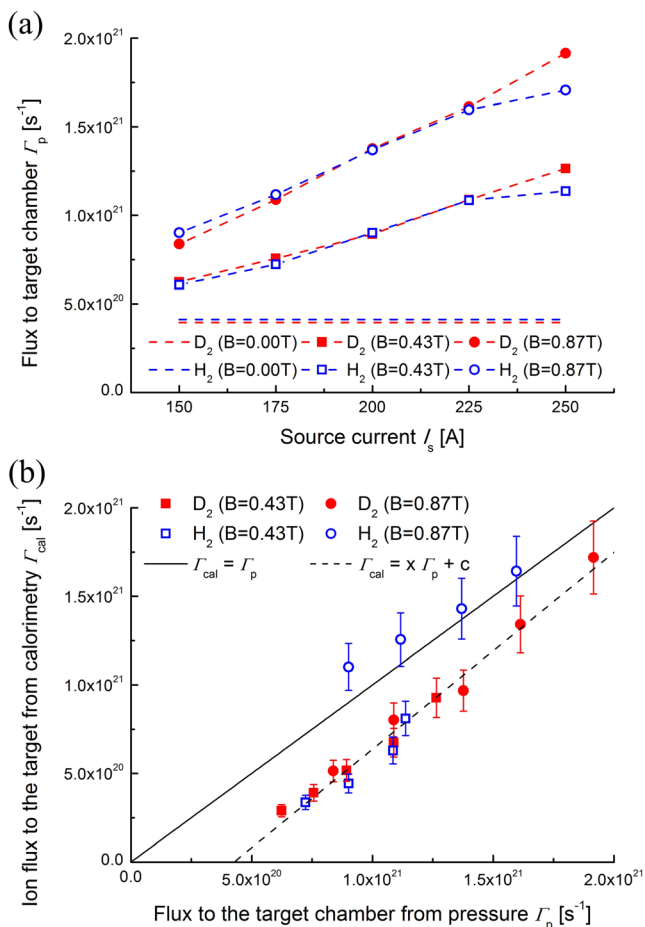ation energy on the other hand was fully taken into account since, for absorption as well as for reflection, the probability for neutralization is very large. In the analysis, we have assumed that the electron and ion temperatures were equal ($T_e = T_i$), which were verified experimentally for similar exposure conditions as used here.[17]

In Fig. 4(b), the ion flux to the target as determined from calorimetry Γ_{cal} is shown as function of the particle flux to the target chamber Γ_p as obtained from the pressure measurements. Except the values for H_2 at $B = 0.87\,\mathrm{T}$, the data points follow a linear trend. The estimated error in Γ_{cal} is a combination in the uncertainties of the calorimetric measurement and the determination of an average T_e for all particles. The estimated error in Γ_p is smaller than the symbol size. The dashed line represents a linear least-squares fit to the data points, excluding the deviating points. The fit intercepts the horizontal axis at a flux of $4.3 \times 10^{20}\,\mathrm{s}^{-1}$, which is very close to the fluxes found without magnetic field (Fig. 4(a)). The solid line illustrates the situation where the ion flux to the target is taken identical to the flow to the target chamber ($\Gamma_{cal} = \Gamma_p$). The conditions at the ITER divertor are represented by this line: the total flux being by far dominated by the ion flux. The fit to the measured data points has an offset to the solid line which slightly decreases for higher fluxes. Concerning the deviating results for H_2 at $B = 0.87\,\mathrm{T}$, all four data points seem to be shifted with respect to the other experimental results. This shift may be related to the target potential during the experiments that was measured to be significantly lower for all four data points (gradually changing from $-45\,\mathrm{V}$ to $-25\,\mathrm{V}$ with increasing current instead of the rather constant values in the range of $-10\,\mathrm{V}$ to $0\,\mathrm{V}$ for all other data points). Although, we are not sure about the exact cause of the shift, an important conclusion valid for all data at higher fluxes can be drawn from Fig. 4(b): the PSI at the target is dominated by the incoming ions and *not* by neutrals coming from the plasma source, thereby approaching the ITER divertor conditions very well.

The average ion flux density and average power flux density to the target can be estimated by dividing the total ion flux, respectively, the total power to the target, by the beam area. We made a conservative estimate with a beam diameter of twice the standard deviation of a Gaussian fit to the n_e profile. This yields average ion flux densities of $\sim 10^{24}\,\mathrm{m}^{-2}\,\mathrm{s}^{-1}$ and average energy flux densities in excess of $4\,\mathrm{MW\,m}^{-2}$. These conditions are similar as what is expected for the strike zones of the ITER divertor. It should be noted that in the center of the target the peak power flux densities are significantly higher and well in excess of $10\,\mathrm{MW\,m}^{-2}$.

Having shown that n_e and T_e in the plasma, and the heat and particle fluxes to the target are close to the ones expected at the ITER divertor, as well as that the PSI is dominated by the incoming ions, another question to have ITER divertor conditions is whether or not we are in the strongly coupled regime. For this to occur, it is essential that the plasma beam diameter is sufficiently large to confine the particles that come off the target, and that the magnetic field is strong enough. The light particles will be confined as soon as they are ionized (Larmor radius $\sim 2\,\mathrm{mm}$). For H and D, the upper limit of the ionization length can be estimated. If we consider a fast reflected H particle with a kinetic energy of

FIG. 4. Flux to the target chamber as a function of source current I_s (a) and comparison between the ion flux to the target determined from calorimetry Γ_{cal} and the total gas flux to the target chamber determined from the pressure measurements Γ_p (b). The H_2 and D_2 flow was $5\,\mathrm{Pa\,m}^3\,\mathrm{s}^{-1}$.

$5T_e \sim 15$ eV,[18] it will have a speed of $\sim 5 \times 10^4$ m s^{-1}. With a charge exchange reaction rate[19] of $\sim 2 \times 10^{-14}$ m^3 s^{-1} and a density $\sim 10^{20}$ m^{-3}, the mean free path for ionization becomes 25 mm. Similar arguments hold for D, leading to a mean free path for ionization of 15 mm. These mean free paths for the fastest particles are comparable to the diameter of the plasma beam. Since the slower particles have smaller mean free paths, this indicates that we have entered the strongly coupled regime for light particles. It should be noted that the direct ionization rates are roughly an order of magnitude lower than the above mentioned charge exchange reaction rate, indicating that the role of recycling is limited for these conditions.

Finally, the total ion flux normalized to the gas flow inserted in the plasma source yields the total ionization efficiency of the linear plasma device. For the highest achieved ion flux of 1.7×10^{21} s^{-1} (see Fig. 4(b)) normalized to the total gas flow of 5 Pa m^3 s^{-1} (which equals 2.7×10^{21} s^{-1} D or H particles), a total ionization efficiency of 63% is reached. This is an unprecedented high value for a steady-state cascaded arc source and more than a factor of two higher than achieved in Pilot-PSI.[20] We attribute this high efficiency to low transport losses due to the low background pressure.

We conclude that the plasma conditions relevant for the ITER divertor strike zones have been reached in the linear plasma generator Magnum-PSI. Thomson scattering just in front of the target yielded electron densities up to 3.6×10^{20} m^{-3} and electron temperatures up to 3.7 eV for H$_2$ and D$_2$ plasmas. The average heat and particle flux densities on the target are well in excess of 4 MW m^{-2} and 10^{24} m^{-2} s^{-1}, respectively. Using pressure and calorimetric measurements, we have shown that the PSI near the target is mainly determined by the incoming ion flux and not by neutrals from the plasma source. The application of a differentially pumped vacuum vessel has led to an unprecedented high ionization efficiency of 63%.

[1]G. Federici, P. Andrew, P. Barabaschi, J. Brooks, R. Doerner, A. Geier, A. Herrmann, G. Janeschitz, K. Krieger, A. Kukushkin, A. Loarte, R. Neu, G. Saibene, M. Shimada, G. Strohmayer, and M. Sugihara, J. Nucl. Mater. **313–316**, 11 (2003).

[2]A. S. Kukushkin, H. D. Pacher, A. Loarte, V. Komarov, V. Kotov, M. Merola, G. W. Pacher, and D. Reiter, Nucl. Fusion **49**, 075008 (2009).

[3]A. Loarte, B. Lipschultz, A. S. Kukushkin, G. F. Matthews, P. C. Stangeby, N. Asakura, G. F. Counsell, G. Federici, A. Kallenbach, K. Krieger, A. Mahdavi, V. Philipps, D. Reiter, J. Roth, J. Strachan, D. Whyte, R. Doerner, T. Eich, W. Fundamenski, A. Herrmann, M. Fenstermacher, P. Ghendrih, M. Groth, A. Kirschner, S. Konoshima, B. LaBombard, P. Lang, A. W. Leonard, P. Monier-Garbet, R. Neu, H. Pacher, B. Pegourie, R. A. Pitts, S. Takamura, J. Terry, and E. Tsitrone, Nucl. Fusion **47**, S203 (2007).

[4]H. Maecker, Z. Naturforsch. **11a**, 457 (1956).

[5]G. M. W. Kroesen, D. C. Schram, and M. J. F. van de Sande, Plasma Chem. Plasma Process. **10**, 49 (1990).

[6]M. C. M. van de Sanden, G. M. Janssen, J. M. de Regt, D. C. Schram, J. A. M. van der Mullen, and B. van der Sijde, Rev. Sci. Instrum. **63**, 3369 (1992).

[7]H. J. N. van Eck, W. R. Koppers, G. J. van Rooij, W. J. Goedheer, R. Engeln, D. C. Schram, N. J. Lopes Cardozo, and A. W. Kleyn, J. Appl. Phys. **105**, 063307 (2009).

[8]G. J. van Rooij, V. P. Veremiyenko, W. J. Goedheer, B. de Groot, A. W. Kleyn, P. H. M. Smeets, T. W. Versloot, D. G. Whyte, R. Engeln, D. C. Schram, and N. J. Lopes Cardozo, Appl. Phys. Lett. **90**, 121501 (2007).

[9]W. L. Hsu, M. Yamada, and P. J. Barrett, Phys. Rev. Lett. **49**, 1001 (1982).

[10]M. G. Rusbridge, G. Sewell, H. Qaosim, D. A. Forder, M. Kay, A. Randewich, A. Mirarefin, P. K. Browning, K. J. Gibson, and J. Hugill, Plasma Phys. Controlled Fusion **42**, 579 (2000).

[11]E. M. Hollmann, A. Yu. Pigarov, R. Seraydarian, D. G. Whyte, and S. I. Krasheninnikov, Phys. Plasmas **9**, 1226 (2002).

[12]M. Ono, A. Tonegawa, K. Kumita, T. Shibuya, and K. Kawamura, J. Nucl. Mater. **337–339**, 261 (2005).

[13]H. J. van der Meiden, A. R. Lof, M. A. van den Berg, S. Brons, A. J. H. Donné, H. J. N. van Eck, P. M. J. Koelman, W. R. Koppers, O. G. Kruijt, N. N. Naumenko, T. Oyevaar, P. R. Prins, J. Rapp, J. Scholten, D. C. Schram, P. H. M. Smeets, G. van der Star, S. N. Tugarinov, and P. A. Zeijlmans van Emmichoven, "Advanced Thomson scattering system for the divertor simulator Magnum-PSI," Rev. Sci. Instrum. (in press).

[14]H. J. N. van Eck, T. A. R. Hansen, A. W. Kleyn, H. J. van der Meiden, D. C. Schram, and P. A. Zeijlmans van Emmichoven, Plasma Sources Sci. Technol. **20**, 045016 (2011).

[15]P. C. Stangeby, *The Plasma Boundary of Magnetic Fusion Devices* (Taylor & Francis Group, London, 2000), p. 69.

[16]W. Eckstein and J. P. Biersack, Appl. Phys. A **38**, 123 (1985).

[17]A. E. Shumack, V. P. Veremiyenko, D. C. Schram, H. J. de Blank, W. J. Goedheer, H. J. van der Meiden, W. A. J. Vijvers, J. Westerhout, N. J. Lopes Cardozo, and G. J. van Rooij, Phys. Rev. E **78**, 046405 (2008).

[18]P. C. Stangeby, *The Plasma Boundary of Magnetic Fusion Devices* (Taylor & Francis Group, London, 2000), p. 94.

[19]J. K. Janev, W. D. Langer, K. Evans, Jr., and D. E. Post, Jr., *Elementary Processes in Hydrogen-Helium Plasmas* (Springer-Verlag, 1987), p. 129.

[20]W. A. J. Vijvers, D. C. Schram, A. E. Shumack, N. J. Lopes Cardozo, J. Rapp, and G. J. van Rooij, Plasma Sources Sci. Technol. **19**, 065016 (2010).